Biophysical Chemistry 159 (2011) 6–13

Contents lists available at ScienceDirect

Biophysical Chemistry

journal homepage: http://www.elsevier.com/locate/biophyschem

Rigidification of the autolysis loop enhances Na^+ binding to thrombin

Nicola Pozzi, Raymond Chen, Zhiwei Chen, Alaji Bah, Enrico Di Cera *

Department of Biochemistry and Molecular Biology, Saint Louis University School of Medicine, St. Louis, MO 63104, USA

ARTICLE INFO

Article history:
Received 15 March 2011
Received in revised form 4 April 2011
Accepted 4 April 2011
Available online 12 April 2011

Keywords:
Thrombin
Na^+ binding
Allostery
X-ray crystallography

ABSTRACT

Binding of Na^+ to thrombin ensures high activity toward physiological substrates and optimizes the procoagulant and prothrombotic roles of the enzyme *in vivo*. Under physiological conditions of pH and temperature, the binding affinity of Na^+ is weak due to large heat capacity and enthalpy changes associated with binding, and the $K_d = 80$ mM ensures only 64% saturation of the site at the concentration of Na^+ in the blood (140 mM). Residues controlling Na^+ binding and activation have been identified. Yet, attempts to improve the interaction of Na^+ with thrombin and possibly increase catalytic activity under physiological conditions have so far been unsuccessful. Here we report how replacement of the flexible autolysis loop of human thrombin with the homologous rigid domain of the murine enzyme results in a drastic (up to 10-fold) increase in Na^+ affinity and a significant improvement in the catalytic activity of the enzyme. Rigidification of the autolysis loop abolishes the heat capacity change associated with Na^+ binding observed in the wild-type and also increases the stability of thrombin. These findings have general relevance to protein engineering studies of clotting proteases and trypsin-like enzymes.

1. Introduction

It is a privilege to contribute to this special issue of Biophysical Chemistry celebrating 25 years of the Gibbs Conference on Biothermodynamics. The corresponding author is deeply indebted to his mentors Dr. Stanley J. Gill, one of the founders of the Gibbs Conference, and Dr. Jeffries Wyman who brought the rigor of thermodynamics to the study of biological macromolecules [1]. Through his training and the many interactions with outstanding scientists attending regularly the Gibbs Conference, the author was able to develop an approach to the study of thrombin and related clotting proteases rooted on the principles of linkage thermodynamics.

Thrombin is a trypsin-like protease endowed with important physiological functions that are mediated and regulated by interaction with numerous macromolecular substrates, receptors and inhibitors [2–4]. Activity of the enzyme toward synthetic and physiological substrates is enhanced allosterically by the binding of Na^+ to a site located >15 Å away from residues of the catalytic triad H57, D102 and S195 [5,6]. The effect of Na^+ is seen not only on cleavage of fibrinogen and PAR1 [7–9], the primary procoagulant and prothrombotic substrates [2,10,11], but also on PAR3 and PAR4 [3,12] and activation of factors V [13], VIII [14] and XI [15] that ensure the build-up of coagulation factors responsible for generation of thrombin from prothrombin [16,17]. Importantly, Na^+ binding has no effect on protein C activation in the absence or presence of thrombomodulin [8,9], which makes Na^+ an exquisite procoagulant cofactor of thrombin. Several naturally occurring mutations of prothrombin [18–23] affect residues linked to Na^+ binding [6] and are associated with bleeding. Furthermore, anticoagulant thrombin mutants have been engineered rationally by perturbing the Na^+ site [9,24–29]. The remarkable success in preclinical studies [27,30–32] indicates that such mutants may soon offer viable alternatives to heparin [29,33,34]. Hence, advances in our basic knowledge of the thrombin–Na^+ interaction have a direct bearing on the pro- and anti-coagulant functions of the enzyme, carry clinical relevance and impact on the treatment of thrombotic disorders.

Na^+ binds 16–20 Å away from residues of the catalytic triad (H57, D102, S195) and within 5 Å from D189 in the primary specificity pocket, nestled between the 220- and 186-loops and coordinated octahedrally by the backbone O atoms of R221a and K224 and four buried water molecules anchored to the side chains of D189, D221 and the backbone atoms of G223 and Y184a [5,6]. The site is highly specific for Na^+ that binds with significantly (>10-fold) higher affinity compared with Li^+, K^+ or Rb^+ [35]. Following the discovery of the role of residue 225 in trypsin-like proteases [36], a Na^+ binding site analogous to the one first identified in thrombin [5] has been documented structurally in factor Xa [37,38], factor VIIa [39] and activated protein C [40]. Identification of the Na^+ binding site of factor IXa remains controversial [41]. Several groups have shown that Na^+ has a significant effect on the activity of factors VIIa [36,42], IXa [43,44], Xa [45–51] and activated protein C [52–56]. Also, in factors IXa [43], Xa [45,46,48–51] and activated protein C [52] the binding of Na^+ influences the primary specificity pocket and is linked to the

* Corresponding author. Tel.: +1 314 977 9201; fax: +1 314 977 1183.
E-mail address: enrico@slu.edu (E. Di Cera).

0301-4622/$ – see front matter © 2011 Elsevier B.V. All rights reserved.
doi:10.1016/j.bpc.2011.04.003

binding of Ca^{2+} to the 70-loop. The physiological role of Na^+ in these enzymes, however, remains unclear and more studies are necessary to verify that Na^+ affects only slightly the activity of the prothrombinase complex [45], has a small [43] or negligible [44] effect on the intrinsic Xase complex and no effect on the extrinsic Xase complex [44].

Na^+ binding to thrombin has been studied in great detail in terms of mutagenesis [6,35,57–59], structure [6], kinetics [57,60,61] and functional components [3,62,63]. Recent studies of rapid and ultra-rapid kinetics [60,61] have revealed the precise mechanism of Na^+ binding to thrombin and uncovered a basic property of the trypsin fold. Na^+ binding to thrombin gives rise to two kinetic phases: one fast (in the microsecond time scale) due to Na^+ binding to the low activity form E to produce the high activity form E:Na^+[60,61], and a second phase considerably slower (in the millisecond time scale) that reflects a pre-equilibrium between E and the inactive form E* according to the kinetic scheme [3,57,60].

The Na^+-free form of thrombin, originally defined as the "slow" form [63], is a mixture of E* and E that interconvert with kinetic rate constants k_r and k_{-r}. Of these forms, E interacts with Na^+ with a rate constant k_A to populate the Na^+-bound form E:Na^+, originally defined as the "fast" form [63], that may dissociate into the parent components with a rate constant k_{-A}. The E*–E–E:Na^+ equilibria also exist in other Na^+-activated enzymes like meizothrombin desF1 [64,65], activated protein C and factor Xa [66]. Several crystal structures of free thrombin have documented the E* form with the Na^+ site and active site blocked [28,57,67,68], and the E form with the active site fully accessible to substrate [6,69,70]. Under physiological conditions, the E:Na^+ form is about 60% of the total and thrombin is almost fully optimized for activity toward fibrinogen and PAR1. When Na^+ is removed from the buffer, thrombin partitions almost equally between E* and E, thereby reducing its activity from high (E:Na^+) to low (E). However, any effect that stabilizes E* over E has the potential to completely abrogate activity. This could explain the bleeding phenotype observed in several mutations of prothrombin [18–23] and the mechanism of action of anticoagulant thrombin mutants [28,71]. If the mutation stabilizes the E* form, activity toward substrate becomes vanishingly small. On the other hand, stabilization of E:Na^+ affords the opposite effect and brings about an increase in catalytic activity. Although evidence of stabilization of E* by specific mutations is now overwhelming [28,57,67,68], no mutation has been reported so far that stabilizes E:Na^+ by increasing the affinity of Na^+ binding. One such mutant is reported here for the first time.

2. Materials and methods

A human thrombin chimera was constructed, expressed and purified to homogeneity as described [6,9,35] using the QuikChange site-directed mutagenesis kit from Stratagene (La Jolla, CA) in a HPC4-modified pNUT expression vector containing the human prethrombin-1 gene. The chimera had the autolysis loop of human thrombin ^{145}KETWTANVGKG^{150} replaced by the analogous sequence ^{145}RETWTTNINEI^{150} in the murine enzyme (six replacements total).

Limited proteolysis of thrombin wild-type and chimera (100 μl, 0.2 mg/ml) was carried out with chymotrypsin for 120 min at 25 °C at a protease/substrate ratio of 1:150 (w/w) using 20 mM Tris, pH 7.4, containing 0.2 M choline chloride (ChCl) or NaCl. Samples taken at different time intervals were mixed immediately with reducing SDS-loading buffer and heated for 3 min at 100 °C. SDS electrophoresis was performed with a 4–12% gradient gel (Invitrogen, CA) and proteins were stained with Coomassie Brilliant Blue R-250.

Urea-mediated denaturation experiments were carried out at 25 ± 0.1 °C, pH 8.0, in the presence of 0.2 M chloride salts as described [72]. After 2 h incubation at the specified urea concentration, protein samples (2 ml, 50 nM) were excited at 280 nm and the fluorescence intensity was recorded at 341 nm. At each urea concentration, the fluorescence signal was adjusted for the corresponding baseline. Data were analyzed within the framework of a two-state process according to the expression

$$F = \frac{F_{0,N} + c_N[D] + F_{0,U} + c_U[D]\exp\left[\frac{m\left([D]-[D]_{1/2}\right)}{RT}\right]}{1 + \exp\left[\frac{m\left([D]-[D]_{1/2}\right)}{RT}\right]} \quad (1)$$

where F is the observed spectroscopic signal at the specified denaturant concentration, $[D]$, $F_{0,N}$ and $F_{0,U}$ are the signal characteristic of the native, N, or unfolded, U, state, c_N and c_U are the baseline slopes for the pre- and post-transition regions, $[D]_{1/2}$ is the urea concentration at which the protein is half unfolded, and m is the slope of the denaturation curve in the transition region. The error on $[D]_{1/2}$ was always <0.1 M urea.

Values of k_{cat}/K_m for hydrolysis of the chromogenic substrates H-D-Phe-Pro-Phe-*p*-nitroanilide (FPF), H-D-Phe-Pro-Lys-*p*-nitroanilide (FPK), H-D-Phe-Pro-Arg-*p*-nitroanilide (FPR), and hydrolysis of the physiological substrates fibrinogen, PAR1 and protein C in the presence of 100 nM thrombomodulin and 5 mM $CaCl_2$ were determined as detailed elsewhere [9,73,74]. Experimental conditions for the studies on chromogenic and physiological substrates were 10 mM Bis-Tris Propane, 0.1% PEG8000, pH 7.4 at 37 °C, in the presence of 145 mM NaCl or ChCl.

Equilibrium dissociation constants for Na^+ binding were determined by fluorescence titration under condition of 10 mM Bis-Tris Propane, 0.1% PEG8000, pH 7.4, 600 mM ionic strength in the temperature range 2–37 °C as detailed elsewhere [75,76]. The temperature dependence of the apparent Na^+ binding constant, K_{app}, was used to derive the thermodynamic parameters associated with the process according to the equation

$$-\ln K_{app} = \frac{\Delta H_0}{R}\frac{1}{T} - \frac{\Delta S_0}{R} + \frac{\Delta C_p}{R}\left(1 - \frac{T}{T_0} - \ln\frac{T}{T_0}\right) \quad (2)$$

where ΔH_0 and ΔS_0 are the enthalpy and entropy changes due to Na^+ binding at the reference temperature $T_0 = 298.15$ K, ΔC_p is the heat-capacity change, R the gas constant and T the absolute temperature. The van't Hoff plot of $-\ln K_{app}$ vs. $1/T$ is linear when $\Delta C_p = 0$ and curves upward when $\Delta C_p < 0$. Stopped-flow measurements were carried out with an Applied Photophysics SX20 spectrometer, with excitation at 280 nm and cutoff filter at 305 nm as described [60,66]. Samples of the protein at a final concentration of 100 nM in a buffer 50 mM Tris, 0.1% PEG8000, pH 8.0 at 15 °C were mixed with an equal volume (60 μl) of buffer containing variable amounts of NaCl. The kinetic traces were analyzed using Scheme 1 with the k_{obs} of the single exponential slow phase due to the E*–E interconversion obeying the expression [60,66]

$$k_{obs} = k_r + k_{-r}\frac{1}{1 + K_A[Na^+]} \quad (3)$$

where K_A is the intrinsic Na^+ affinity related to the apparent binding constant K_{app} by the expression $K_{app} = K_A/(1 + r)$, where $r = k_{-r}/k_r = [E^*]/[E]$ is the equilibrium constant for the E*–E interconversion.

Crystallization was achieved at 22 °C using the hanging drop vapor diffusion method, with each reservoir containing 500 μl of solution. Equal volumes (2.5 μl) of the protein sample (8 mg/ml) in 20 mM Tris,

$$E^* \underset{k_r}{\overset{k_{-r}}{\leftrightarrows}} E \underset{k_A[Na^+]}{\overset{k_{-A}}{\leftrightarrows}} E{:}Na^+$$

Scheme 1.

Table 1
Crystallographic data for the thrombin chimera.

Buffer	0.1 M MES, pH 6.5
PEG	20,000 (20%)
PDB ID	3R3G
Data collection	BIOCARS 14-BM-C
Wavelength (Å)	0.9
Space group	*C*2
Unit cell dimensions (Å)	$a=116.1$ $b=48.1$ $c=53.7$ $\beta=92.1°$
Molecules/asymmetric unit	1
Resolution range (Å)	40–1.75
Observations	101,140
Unique observations	29,518
Completeness (%)	98.3 (97.3)
R_{sym} (%)	6.2 (39.6)
$I/\sigma(I)$	19.1 (2.2)
Refinement	REFMAC
Resolution (Å)	40–1.75
R_{cryst}, R_{free}	0.184, 0.222
Reflections (working/test)	26,527/1495
Protein atoms	2284
Solvent molecules	274
Na^+	2
Rmsd bond lengths[a] (Å)	0.011
Rmsd angles[a] (°)	1.3
Rmsd ΔB (Å^2) (mm/ms/ss)[b]	1.20/1.03/2.32
$\langle B\rangle$ protein (Å^2)	30.5
$\langle B\rangle$ solvent (Å^2)	43.1
$\langle B\rangle$ Na^+ (Å^2)	31.1
Ramachandran plot	
Most favored (%)	99.6
Generously allowed (%)	0.4
Disallowed (%)	0.0

[a] Root-mean-squared deviation (Rmsd) from ideal bond lengths and angles and Rmsd in B-factors of bonded atoms.
[b] mm, main chain–main chain; ms, main chain–side chain; ss, side chain–side chain.

50 mM ChCl, pH 7.4 and reservoir solution (see Table 1) were mixed to prepare the hanging drops. Diffraction quality crystals grew in 2 weeks and were frozen using 25% glycerol as cryoprotectant at 100 K. X-ray diffraction data were collected to 1.75 Å on a Quantum 315 CCD detector at Beamline 14BMC at the Advanced Photon Source, Argonne National Laboratory (Argonne, IL) and were indexed, integrated and scaled with the HKL2000 software package [77]. The structure was solved by molecular replacement using MOLREP from the CCP4 suite [78] and PDB accession code 1SHH as a search model. Refinement and electron density generation were performed with REFMAC [79] from the CCP4 suite and 5% of the reflections were randomly selected as a test set for cross-validation. Model building was performed in COOT [80]. In the final stage of refinement, TLS tensors modeling rigid-body anisotropic temperature factors were calculated and applied to the model. Ramachandran plots were calculated using PROCHECK [81]. Statistics for data collection and refinement are summarized in Table 1. Atomic coordinates and structure factors have been deposited in Protein Data Bank (PDB ID 3R3G).

3. Results

The autolysis loop of thrombin encompasses the sequence ^{145}KETWTANVGKG^{150} and is strategically located between the Na^+ binding site and exosite 1. The loop features a five residue insertion relative to trypsin and chymotrypsin, i.e., ^{149a}ANVGK^{149e}, and is conserved only in length but not in sequence in thrombins from different species [9]. The role of this loop has long remained puzzling because its conformation is highly disordered in existing crystal structures and influenced by packing conditions. However, evidence exists that binding of ligands to exosite I or to the Na^+ site order and rigidify the loop [62,82] and generate a more active enzyme, whereas deletion of the entire segment ^{146}ETWTANVGK^{149e} turns thrombin into an anticoagulant [83] by stabilizing the E* form [28]. Crystallographic data show that the autolysis loop is important in the recognition of PAR4 [84]. Hence, the autolysis loop may play a key role in thrombin function, in contrast to the high degree of disorder documented by crystal structures.

The autolysis loop sequence differs between human and murine thrombin in six amino acid positions. Two substitutions, K145R and V149cI, are conservative. The A149aT substitution introduces a methyl group and a potential H-bond donor. The replacement of ^{149d}GKG^{150} with ^{149d}NEI^{150} inverts the charge ratio of the polypeptide sequence from +1 to −1 and reduces the accessible conformational space. Interest in the murine autolysis loop sequence ^{145}RETWTTNI-NEI^{150} comes from the peculiar functional properties of murine thrombin that lacks Na^+ activation, but retains high catalytic activity toward physiologic substrates because it is locked in the E:Na^+ form [85,86]. The Na^+ activation mimicry is largely due to the D222K substitution [85] and provides a relevant comparison to actin, that folds similarly to the K^+-activated enzyme Hsc70 [87] but uses K18 to replace K^+ in the interaction with the Pα and Pβ of ADP. The side chain of K222 in murine thrombin seals the entrance to the Na^+ site [86], abrogates sensitivity to monovalent cations [85] and generates an environment within the primary specificity pocket that is optimized for substrate binding. However, the inverse substitution D222K in human thrombin abolishes Na^+ activation but does not confer the construct a high catalytic activity comparable to that of the murine enzyme. We therefore turned our attention to the autolysis loop adjacent to the Na^+ site in the hope that it would hold some of the peculiar properties featured by murine thrombin.

Stability studies reveal an unanticipated feature of murine thrombin that is partially recapitulated by the chimera (Fig. 1). Murine thrombin shows a significantly higher stability compared to the human enzyme and the chimera fits in between human and murine wild-type enzymes. Stability of the chimera resembles that of the Na^+-bound form of human thrombin in the absence of Na^+, but is similar to that of murine thrombin in the presence of Na^+. Hence, grafting the

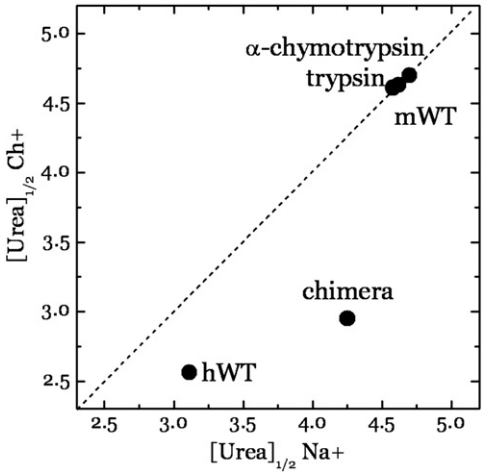

Fig. 1. Role of the autolysis loop on thrombin stability. The value of $[urea]_{1/2}$ necessary to unfold 50% of the enzyme in ChCl is plotted vs. the analogous value in NaCl. The stabilizing effect of Na^+ on wild-type and chimera is evident from the plot, and so is the much higher stability of murine thrombin compared to the human enzyme and its lack of response to Na^+. The values for chymotrypsin and trypsin are also shown for comparison. Analysis of denaturation curves according to Eq. (1) in the text gives the following best-fit values for $[urea]_{1/2}$: (NaCl) 3.11 M (human thrombin), 4.25 M (chimera), 4.58 (murine thrombin), 4.71 M (chymotrypsin), 4.62 M (trypsin); (ChCl) 2.56 M (human thrombin), 2.95 M (chimera), 4.61 (murine thrombin), 4.70 M (chymotrypsin), 4.63 M (trypsin). Errors are 1–2% of the values.

Table 2
Values of k_{cat}/K_m ($\mu M^{-1}\ s^{-1}$) for thrombin wild-type and chimera toward synthetic and physiological substrates.

Enzyme	Cation	FPF	FPK	FPR	FpA	PAR1	PAR3	PAR4	Protein C[a]
wt	Ch^+	0.020 ± 0.001	0.34 ± 0.01	17 ± 1	1.5 ± 0.1	3.0 ± 0.2	0.0085 ± 0.0002	0.049 ± 0.001	0.31 ± 0.01
wt	Na^+	0.49 ± 0.01	4.2 ± 0.1	53 ± 1	16 ± 1	32 ± 1	0.38 ± 0.01	0.35 ± 0.01	0.22 ± 0.01
Chimera	Ch^+	0.089 ± 0.002	1.1 ± 0.1	33 ± 1	5.7 ± 0.1	5.8 ± 0.1	0.049 ± 0.001	0.21 ± 0.01	0.27 ± 0.01
Chimera	Na^+	0.88 ± 0.02	7.3 ± 0.1	122 ± 2	11 ± 1	27 ± 1	0.44 ± 0.01	0.34 ± 0.01	0.19 ± 0.01

FpA: fibrinopeptide A. Experimental conditions are: 10 mM Bis-Tris Propane, 0.1% PEG8000, pH 7.4, 37 °C, 145 mM chloride salt as indicated, plus [a]5 mM $CaCl_2$ and 100 nM thrombomodulin.

autolysis loop of murine thrombin into the human enzymes confers increased stability. The effect is dependent on Na^+, as seen in the human enzyme and in contrast to murine thrombin, thereby indicating that the chimera retains Na^+ binding. Indeed, under physiological conditions of pH and temperature, the catalytic activity of the chimera toward chromogenic substrates measured as k_{cat}/K_m shows a two-fold enhancement relative to wild-type in the presence of Na^+ and an even larger effect in the absence of Na^+ (Table 2). In the case of physiological substrates, fibrinogen, PAR1, PAR3 and PAR4 are cleaved up to 6-fold better by the chimera in the absence of Na^+ but activity is slightly lower in the presence of Na^+. Binding of DAPA to the active site reveals similar signatures in the equilibrium components of ligand recognition (Fig. 2). DAPA binds to the chimera with an affinity almost 2-fold higher than wild-type in the presence of Na^+, but almost 6-fold higher in the absence of Na^+. These observations underscore the important role of the autolysis loop in direct substrate recognition [83] and support the conclusion that the loop assumes a different conformation upon Na^+ binding in the wild-type but is more rigid in the chimera. As a result, access to the active site in the chimera appears to be facilitated, especially in the absence of Na^+.

A direct analysis of Na^+ binding by rapid kinetics reveals a significantly higher Na^+ affinity for the chimera compared to wild-type ($K_A = 350$ vs. $160\ M^{-1}$) (Fig. 3). The amplitude of the slow phase of fluorescence change decreases, vouching for a reduced contribution of the E*–E interconversion in the chimera. The k_{obs} associated with this phase decreases hyperbolically with [Na^+], consistent with the mechanism in Scheme 1, and the asymptotic values are significantly lower than those of wild-type. Best-fit values of k_r and k_{-r} derived from

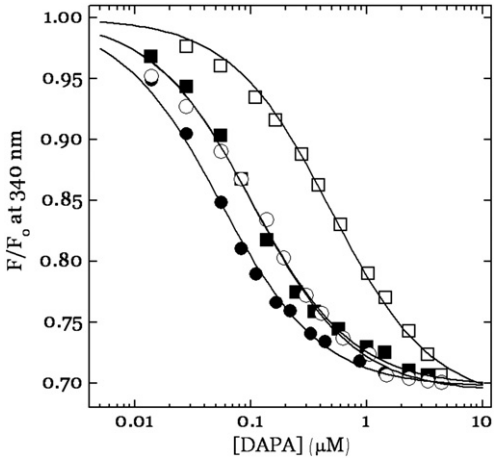

Fig. 2. Binding of DAPA monitored by fluorescence quenching. Experimental conditions are: 50 nM wild-type (open symbols) and 20 nM chimera (closed symbols), 10 mM Bis-Tris Propane, 0.1% PEG8000, pH 7.4 at 37 °C in the presence of 145 mM NaCl (circles) or ChCl (squares). Upon complex formation the total fluorescence decreases up to 30–35%. Best-fit parameters values for the affinity of DAPA are: (wild-type) $K_d = 79 \pm 5$ nM (NaCl), $K_d = 350 \pm 10$ nM (ChCl); (chimera) $K_d = 44 \pm 2$ nM (NaCl), $K_d = 89 \pm 2$ nM (ChCl).

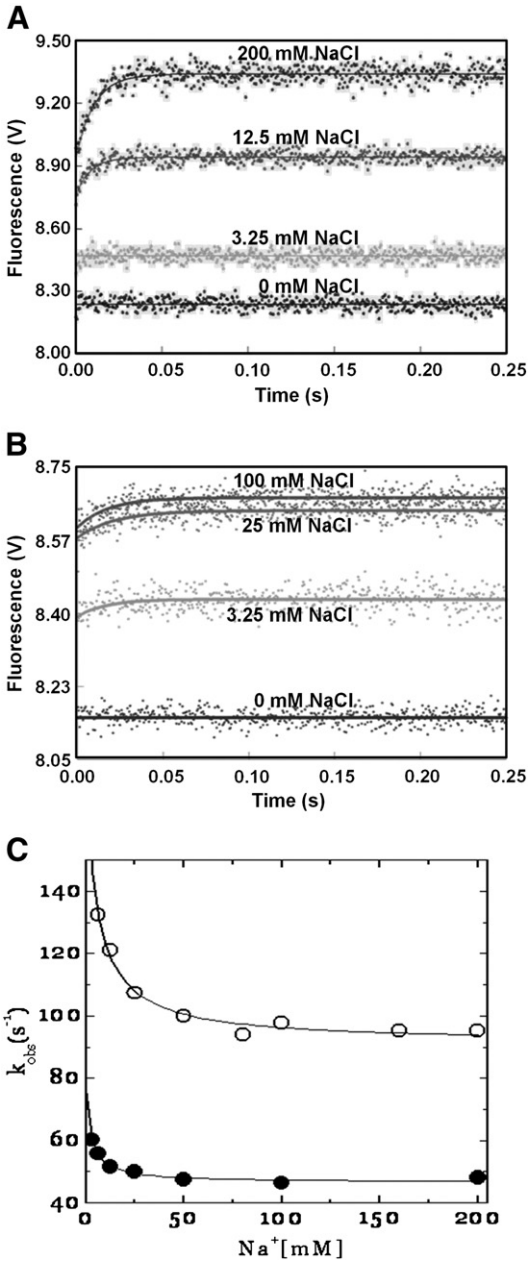

Fig. 3. Kinetic traces of Na^+ binding to thrombin wild-type (A) and chimera (B). In both cases, Na^+ binding obeys a two-step mechanism, with a fast-phase completed within the dead time (<0.5 ms) of the spectrometer, followed by a single-exponential slow phase. Experimental conditions are: 50 nM enzyme, 50 mM Tris, 0.1% PEG8000, pH 8.0 at 15 °C. (C) Values of k_{obs} for the slow phase of fluorescence increase for thrombin wild-type (open circles) and chimera (closed circles). Continuous lines were drawn according to Eq. (3) in the text with best-fit parameters values: (wild-type) $k_r = 91 \pm 2\ s^{-1}$, $k_{-r} = 83 \pm 2\ s^{-1}$, $K_A = 160 \pm 20\ M^{-1}$; (chimera) $k_r = 46 \pm 1\ s^{-1}$, $k_{-r} = 28 \pm 5\ s^{-1}$, $K_A = 350 \pm 30\ M^{-1}$.

analysis of k_{obs} according to Eq. (3) yield $r = k_{-r}/k_r = [E^*]/[E] = 0.60$, which is significantly smaller than the value of 0.92 found in the wild-type. Under the experimental conditions of these rapid kinetic measurements, the population of the E form in the chimera is almost twice as large than that of the E* form, whereas in the wild-type E* and E are almost equally populated. Grafting the autolysis loop of murine thrombin into the human enzyme shifts the E*–E equilibrium in favor of E and increases the intrinsic Na^+ affinity. This observation prompted a more systematic analysis of Na^+ binding.

In the case of wild-type, Na^+ elicits an increase in fluorescence quantum yield of 10–15% [60,63,66,88] and a large negative ΔC_p [75,89] of -860 ± 60 cal/mol/K under physiological conditions (Fig. 4). All nine Trp residues of thrombin are conserved in the chimera, yet the fluorescence baseline signal in ChCl is 5% higher relative to wild-type, suggesting that some fluorophores experience a more hydrophobic environment. Accordingly, binding of Na^+ to the chimera produces only 5–6% enhancement of intrinsic fluorescence. Remarkably, under all experimental conditions tested, the Na^+ binding affinity of the chimera is up to 10-fold higher than that of wild-type. At physiological temperature and $I = 600$ mM, the K_d for Na^+ binding is 109 mM for wild-type but only 20 mM for the chimera (Fig. 4). The van't Hoff plot for Na^+ binding to wild-type shows the expected curvature indicative of a linked negative ΔC_p, but is linear for the chimera over the entire temperature range from 2 to 37 °C. The chimera also shows lower dependence of Na^+ binding on ionic strength as compared to wild-type (Fig. 4). An important consequence of the higher Na^+ affinity of the chimera is revealed by the effect of $[Na^+]$ on the hydrolysis of fibrinogen under physiological conditions of pH, temperature and ionic strength (Fig. 5). In the case of wild-type, Na^+ increases drastically the k_{cat}/K_m for release of fibrinopeptide A from fibrinogen but the physiological $[Na^+] = 140$ mM is not sufficient to saturate the effect. In the case of the chimera, on the other hand, saturation is achieved around $[Na^+] = 60$ mM. In both enzymes, Na^+ has no effect on the hydrolysis of protein C in the presence of Ca^{2+} and thrombomodulin.

The functional data on the chimera strongly suggest that the autolysis loop is a dominant factor controlling the energetics of Na^+ binding to thrombin and also influences the catalytic activity of the enzyme. However, the molecular origin of these effects remains elusive and cannot be anticipated from the difference in sequence between the human and murine loops. The structure of the chimera was therefore solved and crystals were obtained at high resolution (1.75 Å) in the presence of Na^+. The structure is very similar (rmsd = 0.422 Å) to the E:Na^+ form of thrombin [6] (Fig. 6). The catalytic triad is oriented for optimal activity and the specificity sites S1, S2 and S3 are widely accessible to substrate. The 186- and 220-loops defining the Na^+ binding site are in the optimal conformation for Na^+ coordination and the cation is octahedrally bound to four water molecules and the carbonyl O atoms of K224 and R221a as in the wild-type [5]. Because crystals were grown for an active enzyme

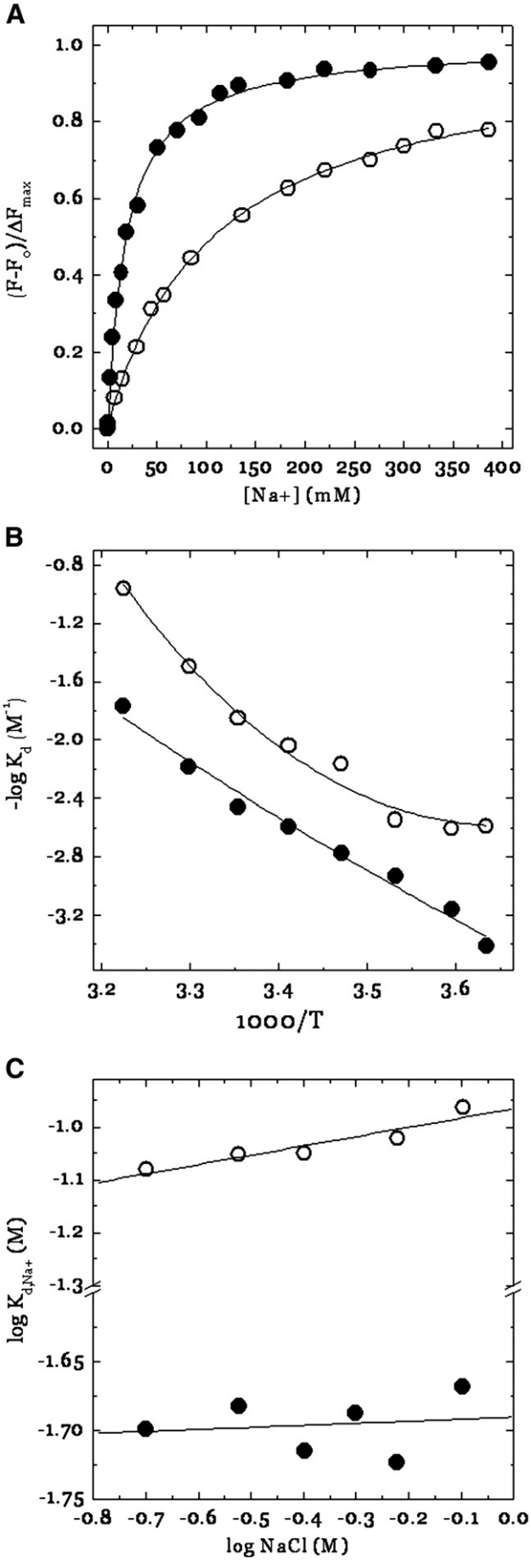

Fig. 4. (A) Na^+ binding to thrombin wild-type (open circles) and chimera (closed circles) monitored by fluorescence spectroscopy. Experimental conditions are: 10 mM Bis-Tris Propane, 0.1% PEG8000, pH 7.4 at 37 °C, $I = 600$ mM. The equilibrium dissociation constant K_d for Na^+ binding is 109 ± 5 mM for wild-type and 20 ± 1 mM for the chimera. (B) van't Hoff plot of Na^+ binding to thrombin wild-type (open circles) and chimera (closed circles). Shown are the values of K_d obtained from fluorescence titration over the temperature range 2–37 °C, under experimental conditions of 80 nM enzyme, 10 mM Bis-Tris Propane, 0.1% PEG8000, pH 7.4, $I = 600$ mM kept constant with ChCl. Excitation and emission wavelengths were 280 and 341 nm, respectively. Continuous lines were drawn according to Eq. (2) in the text with best-fit parameters values: (wild-type) $\Delta H_0 = -23.6 \pm 0.5$ kcal/mol, $\Delta S_0 = -71 \pm 4$ cal/mol/K, $\Delta C_p = -860 \pm 60$ cal/mol/K; (chimera) $\Delta H_0 = -17.4 \pm 0.5$ kcal/mol, $\Delta S_0 = -49 \pm 2$ cal/mol/K, $\Delta C_p = 0$. (C) Effect of ionic strength on the binding of Na^+ to thrombin wild-type (open circles) and chimera (closed circles). Experimental conditions are: 50 mM Tris, 0.1% PEG8000, pH 7.4 at 37 °C. The ionic strength was changed by addition of ChCl. Continuous lines were drawn according to the equation $-\log K_d = A_0 + \Gamma \log[NaCl]$ [89], with best-fit parameter values: (wild-type) $A_0 = 0.96 \pm 0.02$, $\Gamma = -0.19 \pm 0.06$; (chimera) $A_0 = 1.69 \pm 0.04$, $\Gamma = -0.015 \pm 0.005$.

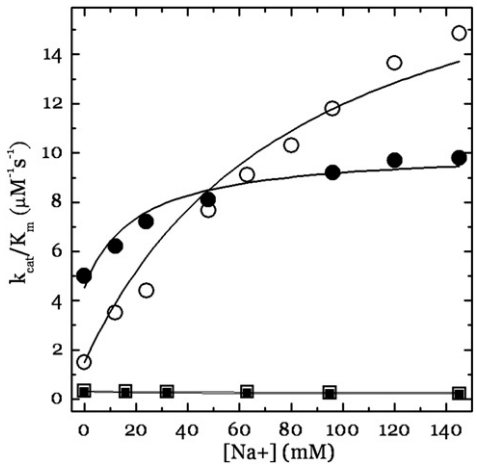

Fig. 5. Effect of Na^+ on the hydrolysis of physiological substrates. Shown is the dependence of k_{cat}/K_m for the cleavage of fibrinogen (circles) and protein C (squares) in the presence of 5 mM Ca^{2+} and 100 nM thrombomodulin for thrombin wild-type (open circles) and chimera (closed circles). Experimental conditions are: 20 mM Tris, 0.1% PEG8000, pH 7.4 at 37 °C. The ionic strength was kept constant at 145 mM with ChCl. Continuous lines were drawn according to the linkage equation $k_{cat}/K_m = s = \frac{s_0 + s_1 K_{app}[Na^+]}{1 + K_{app}[Na^+]}$ [3,57], where s_0 and s_1 are the values of k_{cat}/K_m at $[Na^+]=0$ M and under saturating conditions, with best-fit parameter values: (wild-type, fibrinogen): $s_0 = 1.5 \pm 0.1\ \mu M^{-1}\ s^{-1}$, $s_1 = 21 \pm 2\ \mu M^{-1}\ s^{-1}$, $K_{app} = 12 \pm 1\ M^{-1}$; (chimera, fibrinogen) $s_0 = 4.5 \pm 0.2\ \mu M^{-1}\ s^{-1}$, $s_1 = 10 \pm 1\ \mu M^{-1}\ s^{-1}$, $K_{app} = 50 \pm 2\ M^{-1}$; (wild-type, protein C) $s_0 = 0.32 \pm 0.02\ \mu M^{-1}\ s^{-1}$, $s_1 = 0.20 \pm 0.01\ \mu M^{-1}\ s^{-1}$, $K_{app} = 12 \pm 1\ M^{-1}$; (chimera, protein C) $s_0 = 0.29 \pm 0.01\ \mu M^{-1}\ s^{-1}$, $s_1 = 0.21 \pm 0.03\ \mu M^{-1}\ s^{-1}$, $K_{app} = 50 \pm 10\ M^{-1}$.

in the absence of any inhibitors, exosite I is cleaved at R77a and the entire segment 73–77 is missing in the electron density map. Perturbation of exosite I induces a flip in the orientation of W141, as seen in the murine enzyme [86]. Notably, the autolysis loop in the chimera is well defined in its entirety. The murine sequence 145–150 introduced in the human enzyme is readily traced in the electron density map (Fig. 6) vouching for a more rigid and locked conformation. I149c packs against W148 and stabilizes the indole ring in a way that would not be possible with the Val residue carried at this position by the human enzyme. The hydrophobic interaction is further stabilized by the side chain of I150 that replaces G150 in the human enzyme and penetrates deeply into the loop. The Oδ1 atom of N149d H-bonds to the Nδ2 atom of N149b forcing the backbone to assume a small helix turn. An ion pair between R145 and E18 anchors the N-terminus of the B chain and fixes the geometry of the loop, as previously seen in the murine but not the human enzyme. Altogether, these contacts vouch for increased rigidity of the autolysis loop in the chimera relative to wild-type. Support to this conclusion comes from studies of limited proteolysis that is ideally suited to detect differences in protein flexibility in solution [82,90]. Under the assay conditions used in this study, digestion of thrombin by chymotrypsin mainly takes place at the C-terminal of W148, located right in the middle of the autolysis loop. Fig. 7 shows the time course of the proteolytic reaction monitored by SDS-PAGE. Under reducing conditions, thrombin migrates as heavy chain and light chain, with molecular weights of ~30 and 4 kDa, respectively. After 40 min, more than 80% of the heavy chain of wild-type is cleaved by chymotrypsin but the heavy chain of the chimera appears significantly resistant.

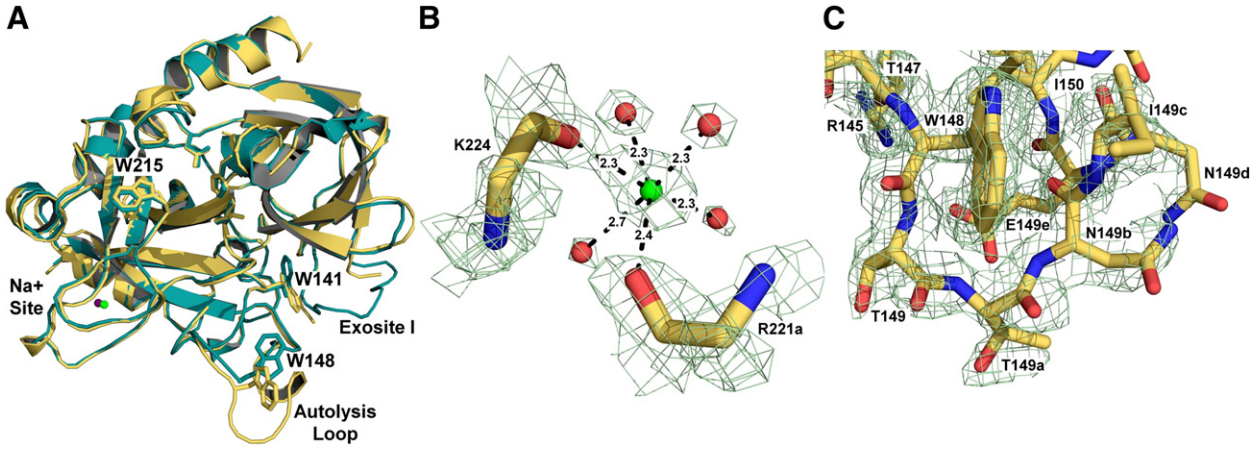

Fig. 6. Crystal structure of the chimera. (A) Superposition of human wild-type thrombin (1SG8, *cyan*) and chimera (3R3G, *gold*) (rmsd = 0.422 Å). Residues of the catalytic triad (H57, D102, S195) and Trp residues reporting the E^*–E–E:Na^+ transitions (W215, W141, W148) [60] are rendered as sticks. Relevant domains of the enzyme are noted. The bound Na^+ is rendered as a sphere. (B) The coordination shell of Na^+ in the chimera is similar to that of wild-type and involves four water molecules and the backbone O atoms of R221a and K224. H-bonding distances are noted. The electron density $2F_0$–F_c map (green) is countered at 1 σ. (C) The autolysis loop of the chimera is stabilized by the hydrophobic cluster composed of W148, I149c and I150, the H-bond between N149b and N149d and a salt bridge between R145 and E18 that anchors the N-terminus of the heavy chain. The electron density $2F_0$–F_c map (green) is countered at 0.7 σ.

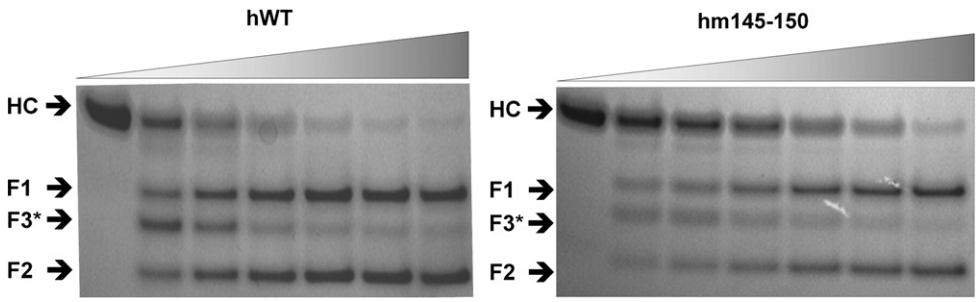

Fig. 7. Flexibility of the autolysis loop probed by limited proteolysis. Thrombin wild-type or chimera was incubated with chymotrypsin using an enzyme/substrate ratio of 1:150 (w/w) under experimental conditions of 20 mM Tris, 200 mM ChCl, pH 7.4. Samples were taken at 0, 5, 10, 20, 40, 60 and 120 min and loaded into a 4–12% gradient gel under reducing conditions. HC is the heavy chain, F1 and F2 are the cleavage products generated by chymotrypsin, encompassing the sequence 36–148 (17 kDa) and 149–259 (10 kDa), respectively. F3* is a secondary product of the reaction that is further proteolyzed by chymotrypsin as a function of time.

4. Discussion

The effect of Na^+ on thrombin can be summarized in terms of three important components. First, Na^+ increases the catalytic activity of the enzyme toward synthetic and physiological substrates, with the exception of the anticoagulant protein C [8,9]. Second, Na^+ binding obeys a two-step mechanism consistent with a pre-existing equilibrium between the inactive form E* and low activity form E, followed by selective binding to E to generate the high activity form E:Na^+ [60]. Third, the affinity of Na^+ is strongly temperature dependent, with a large heat capacity change and enthalpy that cause the K_d to become comparable to the [Na^+] in the blood under physiological conditions [35,89]. The results presented here show, for the first time, that the Na^+ affinity of thrombin can be enhanced by site-directed mutagenesis and offer new insights into the molecular determinants that control Na^+ binding and catalytic activity of the enzyme. Replacement of the highly flexible autolysis loop of human thrombin with the homologous region of murine thrombin produces a chimera with an affinity toward Na^+ up to 10-fold higher than wild-type. Because murine thrombin is constitutively stabilized in the E:Na^+ form [85,86], the chimera affords an important intermediate along the pathway that converts Na^+ activation in the human enzyme into constitutive activation in the murine enzyme. The D222K substitution is a key component of Na^+ mimicry and provides an effective replacement of the bound cation in murine thrombin [85,86]. The autolysis loop bears a total of six substitutions between human and murine enzymes and reveals additional important features. In the crystal structure of the chimera, the loop assumes a highly ordered conformation stabilized by hydrophobic interactions between I149c and W148. As a result of the enhanced rigidity of the loop, the Na^+ affinity is enhanced and so is thermodynamic stability. In addition, Na^+ binding is no longer linked to a large heat capacity change. All these functional features of the chimera lead us to conclude that the autolysis loop of thrombin controls, through its intrinsic flexibility, the affinity toward Na^+, the associated heat capacity change and thermodynamic stability of the enzyme. At the molecular level, this effect is achieved by stabilizing the active E form relative to the inactive E* form and converting E more efficiently to the E:Na^+ form.

The observation that the Na^+ binding site of thrombin is under the influence of the neighbor autolysis loop is intriguing. The thermodynamic origin of the increased Na^+ affinity in the chimera is entirely entropic because under physiological conditions the enthalpy of binding is actually more favorable in the wild-type (Fig. 4). Hence, Na^+ binding to thrombin can be optimized by ordering the autolysis loop that contributes a large entropy loss in the wild-type because of its intrinsic flexibility. This entropy change offsets the large and favorable enthalpy change provided by the coordination shell of Na^+ and together the thermodynamic components of binding result in a modest affinity under physiological conditions that is not sufficient to saturate the site. Rigidification of the autolysis loop also enhances stability and makes human thrombin more similar to the murine enzyme, which is surprisingly more stable. These findings provide an important first step in the design of thrombin variants with improved catalytic activity *in vivo*. They also add considerably to our understanding of the molecular determinants of thrombin function in ways that benefit future engineering studies of clotting enzymes activated by monovalent cations [91,92].

Acknowledgments

This work was supported in part by NIH research grants HL049413, HL058141, HL073813 and HL095315.

References

[1] J. Wyman, S.J. Gill, Binding and Linkage, University Science Books, Mill Valley, CA, 1990.
[2] E.W. Davie, J.D. Kulman, An overview of the structure and function of thrombin, Semin. Thromb. Hemost. 32 (Suppl 1) (2006) 3–15.
[3] E. Di Cera, Thrombin, Mol. Aspects Med. 29 (2008) 203–254.
[4] W. Bode, Structure and interaction modes of thrombin, Blood Cells Mol. Dis. 36 (2006) 122–130.
[5] E. Di Cera, E.R. Guinto, A. Vindigni, Q.D. Dang, Y.M. Ayala, M. Wuyi, A. Tulinsky, The Na+ binding site of thrombin, J. Biol. Chem. 270 (1995) 22089–22092.
[6] A.O. Pineda, C.J. Carrell, L.A. Bush, S. Prasad, S. Caccia, Z.W. Chen, F.S. Mathews, E. Di Cera, Molecular dissection of Na+ binding to thrombin, J. Biol. Chem. 279 (2004) 31842–31853.
[7] Y.M. Ayala, A.M. Cantwell, T. Rose, L.A. Bush, D. Arosio, E. Di Cera, Molecular mapping of thrombin–receptor interactions, Proteins 45 (2001) 107–116.
[8] O.D. Dang, A. Vindigni, E. Di Cera, An allosteric switch controls the procoagulant and anticoagulant activities of thrombin, Proc. Natl. Acad. Sci. USA 92 (1995) 5977–5981.
[9] Q.D. Dang, E.R. Guinto, E. Di Cera, Rational engineering of activity and specificity in a serine protease, Nat. Biotechnol. 15 (1997) 146–149.
[10] S.R. Coughlin, Thrombin signalling and protease-activated receptors, Nature 407 (2000) 258–264.
[11] S.R. Coughlin, Protease-activated receptors in hemostasis, thrombosis and vascular biology, J. Thromb. Haemost. 3 (2005) 1800–1814.
[12] E. Di Cera, Thrombin as procoagulant and anticoagulant, J. Thromb. Haemost. 5 (2007) 196–202.
[13] T. Myles, T.H. Yun, S.W. Hall, L.L. Leung, An extensive interaction interface between thrombin and factor V is required for factor V activation, J. Biol. Chem. 276 (2001) 25143–25149.
[14] K. Nogami, Q. Zhou, T. Myles, L.L. Leung, H. Wakabayashi, P.J. Fay, Exosite-interactive regions in the A1 and A2 domains of factor VIII facilitate thrombin-catalyzed cleavage of heavy chain, J. Biol. Chem. 280 (2005) 18476–18487.
[15] T.H. Yun, F.A. Baglia, T. Myles, D. Navaneetham, J.A. Lopez, P.N. Walsh, L.L. Leung, Thrombin activation of factor XI on activated platelets requires the interaction of factor XI and platelet glycoprotein Ib alpha with thrombin anion-binding exosites I and II, respectively, J. Biol. Chem. 278 (2003) 48112–48119.
[16] K.G. Mann, Thrombin formation, Chest 124 (2003) 4S–10S.
[17] K.G. Mann, S. Butenas, K. Brummel, The dynamics of thrombin formation, Arterioscler. Thromb. Vasc. Biol. 23 (2003) 17–25.
[18] S.J. Degen, S.A. McDowell, L.M. Sparks, I. Scharrer, Prothrombin Frankfurt: a dysfunctional prothrombin characterized by substitution of Glu-466 by Ala, Thromb. Haemost. 73 (1995) 203–209.
[19] T. Miyata, R. Aruga, H. Umeyama, A. Bezeaud, M.C. Guillin, S. Iwanaga, Prothrombin Salakta: substitution of glutamic acid-466 by alanine reduces the fibrinogen clotting activity and the esterase activity, Biochemistry 31 (1992) 7457–7462.
[20] R.A. Henriksen, C.K. Dunham, L.D. Miller, J.T. Casey, J.B. Menke, C.L. Knupp, S.J. Usala, Prothrombin Greenville, Arg517→Gln, identified in an individual heterozygous for dysprothrombinemia, Blood 91 (1998) 2026–2031.
[21] W.Y. Sun, D. Smirnow, M.L. Jenkins, S.J. Degen, Prothrombin Scranton: substitution of an amino acid residue involved in the binding of Na+ (LYS-556 to THR) leads to dysprothrombinemia, Thromb. Haemost. 85 (2001) 651–654.
[22] H. Stanchev, M. Philips, B.O. Villoutreix, L. Aksglaede, S. Lethagen, S. Thorsen, Prothrombin deficiency caused by compound heterozygosity for two novel mutations in the prothrombin gene associated with a bleeding tendency, Thromb. Haemost. 95 (2006) 195–198.
[23] S. Rouy, D. Vidaud, J.L. Alessandri, M.D. Dautzenberg, L. Venisse, M.C. Guillin, A. Bezeaud, Prothrombin Saint-Denis: a natural variant with a point mutation resulting in Asp to Glu substitution at position 552 in prothrombin, Br. J. Haematol. 132 (2006) 770–773.
[24] C.S. Gibbs, S.E. Coutre, M. Tsiang, W.X. Li, A.K. Jain, K.E. Dunn, V.S. Law, C.T. Mao, S.Y. Matsumura, S.J. Mejza, L.R. Paborsky, L.L.K. Leung, Conversion of thrombin into an anticoagulant by protein engineering, Nature 378 (1995) 413–416.
[25] M. Tsiang, L.R. Paborsky, W.X. Li, A.K. Jain, C.T. Mao, K.E. Dunn, D.W. Lee, S.Y. Matsumura, M.D. Matteucci, S.E. Coutre, L.L. Leung, C.S. Gibbs, Protein engineering thrombin for optimal specificity and potency of anticoagulant activity in vivo, Biochemistry 35 (1996) 16449–16457.
[26] A.M. Cantwell, E. Di Cera, Rational design of a potent anticoagulant thrombin, J. Biol. Chem. 275 (2000) 39827–39830.
[27] A. Gruber, A.M. Cantwell, E. Di Cera, S.R. Hanson, The thrombin mutant W215A/E217A shows safe and potent anticoagulant and antithrombotic effects in vivo, J. Biol. Chem. 277 (2002) 27581–27584.
[28] A. Bah, C.J. Carrell, Z. Chen, P.S. Gandhi, E. Di Cera, Stabilization of the E* form turns thrombin into an anticoagulant, J. Biol. Chem. 284 (2009) 20034–20040.
[29] E. Di Cera, Thrombin as an anticoagulant, Prog. Mol. Biol. Transl. Sci. 99 (2011) 145–184.
[30] M.A. Berny, T.C. White, E.I. Tucker, L.A. Bush-Pelc, E. Di Cera, A. Gruber, O.J. McCarty, Thrombin mutant W215A/E217A acts as a platelet GpIb antagonist, Arterioscler. Thromb. Vasc. Biol. 18 (2008) 329–334.
[31] A. Gruber, J.A. Fernandez, L. Bush, U. Marzec, J.H. Griffin, S.R. Hanson, E. Di Cera, Limited generation of activated protein C during infusion of the protein C activator thrombin analog W215A/E217A in primates, J. Thromb. Haemost. 4 (2006) 392–397.
[32] A. Gruber, U.M. Marzec, L. Bush, E. Di Cera, J.A. Fernandez, M.A. Berny, E.I. Tucker, O.J. McCarty, J.H. Griffin, S.R. Hanson, Relative antithrombotic and antihemostatic effects of protein C activator versus low molecular weight heparin in primates, Blood 109 (2007) 3733–3740.
[33] S.M. Bates, J.I. Weitz, The status of new anticoagulants, Br. J. Haematol. 134 (2006) 3–19.
[34] J. Erdmann, Engineered thrombin aims to take on heparin, Chem. Biol. 17 (2010) 1267–1268.
[35] S. Prasad, K.J. Wright, D.B. Roy, L.A. Bush, A.M. Cantwell, E. Di Cera, Redesigning the monovalent cation specificity of an enzyme, Proc. Natl. Acad. Sci. USA 100 (2003) 13785–13790.

[36] Q.D. Dang, E. Di Cera, Residue 225 determines the Na(+)-induced allosteric regulation of catalytic activity in serine proteases, Proc. Natl. Acad. Sci. USA 93 (1996) 10653–10656.
[37] E. Zhang, A. Tulinsky, The molecular environment of the Na+ binding site of thrombin, Biophys. Chem. 63 (1997) 185–200.
[38] K. Scharer, M. Morgenthaler, R. Paulini, U. Obst-Sander, D.W. Banner, D. Schlatter, J. Benz, M. Stihle, F. Diederich, Quantification of cation–pi interactions in protein–ligand complexes: crystal-structure analysis of Factor Xa bound to a quaternary ammonium ion ligand, Angew. Chem. Int. Ed. Engl. 44 (2005) 4400–4404.
[39] S.P. Bajaj, A.E. Schmidt, S. Agah, M.S. Bajaj, K. Padmanabhan, High resolution structures of p-aminobenzamidine- and benzamidine-VIIa/soluble tissue factor: unpredictedconformationofthe 192–193 peptidebondandmappingof Ca2+, Mg2+, Na+, and Zn2+ sitesinfactor VIIa, J. Biol. Chem. 281 (2006) 24873–24888.
[40] A.E. Schmidt, K. Padmanabhan, M.C. Underwood, W. Bode, T. Mather, S.P. Bajaj, Thermodynamic linkage between the S1 site, the Na+ site, and the Ca2+ site in the protease domain of human activated protein C (APC). Sodium ion in the APC crystal structure is coordinated to four carbonyl groups from two separate loops, J. Biol. Chem. 277 (2002) 28987–28995.
[41] T. Zogg, H. Brandstetter, Structural basis of the cofactor- and substrate-assisted activation of human coagulation factor IXa, Structure 17 (2009) 1669–1678.
[42] R.J. Petrovan, W. Ruf, Role of residue Phe225 in the cofactor-mediated, allosteric regulation of the serine protease coagulation factor VIIa, Biochemistry 39 (2000) 14457–14463.
[43] A.E. Schmidt, J.E. Stewart, A. Mathur, S. Krishnaswamy, S.P. Bajaj, Na+ site in blood coagulation factor IXa: effect on catalysis and factor VIIIa binding, J. Mol. Biol. 350 (2005) 78–91.
[44] K. Gopalakrishna, A.R. Rezaie, The influence of sodium ion binding on factor IXa activity, Thromb. Haemost. 95 (2006) 936–941.
[45] A.R. Rezaie, X. He, Sodium binding site of factor Xa: role of sodium in the prothrombinase complex, Biochemistry 39 (2000) 1817–1825.
[46] A.R. Rezaie, F.S. Kittur, The critical role of the 185–189-loop in the factor Xa interaction with Na+ and factor Va in the prothrombinase complex, J. Biol. Chem. 279 (2004) 48262–48269.
[47] C.L. Orthner, D.P. Kosow, The effect of metal ions on the amidolytic activity of human factor Xa (activated Stuart-Prower factor), Arch. Biochem. Biophys. 185 (1978) 400–406.
[48] D. Monnaie, D. Arosio, N. Griffon, T. Rose, A.R. Rezaie, E. Di Cera, Identification of a binding site for quaternary amines in factor Xa, Biochemistry 39 (2000) 5349–5354.
[49] M.C. Underwood, D. Zhong, A. Mathur, T. Heyduk, S.P. Bajaj, Thermodynamic linkage between the S1 site, the Na+ site, and the Ca2+ site in the protease domain of human coagulation factor xa. Studies on catalytic efficiency and inhibitor binding, J. Biol. Chem. 275 (2000) 36876–36884.
[50] R.M. Camire, Prothrombinase assembly and S1 site occupation restore the catalytic activity of FXa impaired by mutation at the sodium-binding site, J. Biol. Chem. 277 (2002) 37863–37870.
[51] S. Levigne, F. Thiec, S. Cherel, J.A. Irving, C. Fribourg, O.D. Christophe, Role of the alpha-helix 163–170 in factor Xa catalytic activity, J. Biol. Chem. 282 (2007) 31569–31579.
[52] X. He, A.R. Rezaie, Identification and characterization of the sodium-binding site of activated protein C, J. Biol. Chem. 274 (1999) 4970–4976.
[53] S.A. Steiner, G.W. Amphlett, F.J. Castellino, Stimulation of the amidase and esterase activity of activated bovine plasma protein C by monovalent cations, Biochem. Biophys. Res. Commun. 94 (1980) 340–347.
[54] S.A. Steiner, F.J. Castellino, Kinetic studies of the role of monovalent cations in the amidolytic activity of activated bovine plasma protein C, Biochemistry 21 (1982) 4609–4614.
[55] S.A. Steiner, F.J. Castellino, Effect of monovalent cations on the pre-steady-state kinetic parameters of the plasma protease bovine activated protein C, Biochemistry 24 (1985) 1136–1141.
[56] S.A. Steiner, F.J. Castellino, Kinetic mechanism for stimulation by monovalent cations of the amidase activity of the plasma protease bovine activated protein C, Biochemistry 24 (1985) 609–617.
[57] W. Niu, Z. Chen, L.A. Bush-Pelc, A. Bah, P.S. Gandhi, E. Di Cera, Mutant N143P reveals how Na+ activates thrombin, J. Biol. Chem. 284 (2009) 36175–36185.
[58] S. Prasad, A.M. Cantwell, L.A. Bush, P. Shih, H. Xu, E. Di Cera, Residue Asp-189 controls both substrate binding and the monovalent cation specificity of thrombin, J. Biol. Chem. 279 (2004) 10103–10108.
[59] S. Rana, N. Pozzi, L.A. Pelc, E. Di Cera, Redesigning allosteric activation in an enzyme, Proc. Natl. Acad. Sci. USA 108 (2011) 5221–5225.
[60] A. Bah, L.C. Garvey, J. Ge, E. Di Cera, Rapid kinetics of Na+ binding to thrombin, J. Biol. Chem. 281 (2006) 40049–40056.
[61] S. Gianni, Y. Ivarsson, A. Bah, L.A. Bush-Pelc, E. Di Cera, Mechanism of Na+ binding to thrombin resolved by ultra-rapid kinetics, Biophys. Chem. 131 (2007) 111–114.
[62] V. De Filippis, E. De Dea, F. Lucatello, R. Frasson, Effect of Na+ binding on the conformation, stability and molecular recognition properties of thrombin, Biochem. J. 390 (2005) 485–492.
[63] C.M. Wells, E. Di Cera, Thrombin is a Na(+)-activated enzyme, Biochemistry 31 (1992) 11721–11730.
[64] M.E. Papaconstantinou, P.S. Gandhi, Z. Chen, A. Bah, E. Di Cera, Na(+) binding to meizothrombin desF1, Cell. Mol. Life Sci. 65 (2008) 3688–3697.
[65] H.K. Kroh, G. Tans, G.A.F. Nicolaes, J. Rosing, P.E. Bock, Expression of allosteric linkage between the sodium ion binding site and exosite I of thrombin during prothrombin activation, J. Biol. Chem. 282 (2007) 16095–16104.
[66] A.D. Vogt, A. Bah, E. Di Cera, Evidence of the E*-E equilibrium from rapid kinetics of Na(+) binding to activated protein C and factor Xa, J. Phys. Chem. B 114 (2010) 16125–16130.
[67] P.S. Gandhi, Z. Chen, F.S. Mathews, E. Di Cera, Structural identification of the pathway of long-range communication in an allosteric enzyme, Proc. Natl. Acad. Sci. USA 105 (2008) 1832–1837.
[68] A.O. Pineda, Z.W. Chen, A. Bah, L.C. Garvey, F.S. Mathews, E. Di Cera, Crystal structure of thrombin in a self-inhibited conformation, J. Biol. Chem. 281 (2006) 32922–32928.
[69] L.A. Bush-Pelc, F. Marino, Z. Chen, A.O. Pineda, F.S. Mathews, E. Di Cera, Important role of the Cys-191: Cys-220 disulfide bond in thrombin function and allostery, J. Biol. Chem. 282 (2007) 27165–27170.
[70] A.O. Pineda, S.N. Savvides, G. Waksman, E. Di Cera, Crystal structure of the anticoagulant slow form of thrombin, J. Biol. Chem. 277 (2002) 40177–40180.
[71] P.S. Gandhi, M.J. Page, Z. Chen, L.A. Bush-Pelc, E. Di Cera, Mechanism of the anticoagulant activity of the thrombin mutant W215A/E217A, J. Biol. Chem. 284 (2009) 24098–24105.
[72] M.R. Eftink, The use of fluorescence methods to monitor unfolding transitions in proteins, Biophys. J. 66 (1994) 482–501.
[73] M.M. Krem, E. Di Cera, Dissecting substrate recognition by thrombin using the inactive mutant S195A, Biophys. Chem. 100 (2003) 315–323.
[74] A. Vindigni, E. Di Cera, Release of fibrinopeptides by the slow and fast forms of thrombin, Biochemistry 35 (1996) 4417–4426.
[75] N. Griffon, E. Di Stasio, Thermodynamics of Na+ binding to coagulation serine proteases, Biophys. Chem. 90 (2001) 89–96.
[76] S. Prasad, K.J. Wright, D. Banerjee Roy, L.A. Bush, A.M. Cantwell, E. Di Cera, Redesigning the monovalent cation specificity of an enzyme, Proc. Natl. Acad. Sci. USA 100 (2003) 13785–13790.
[77] Z. Otwinowski, W. Minor, Processing of X-ray diffraction data collected in oscillation mode, Methods Enzymol. 276 (1997) 307–326.
[78] S. Bailey, The CCP4 suite. Programs for protein crystallography, Acta Crystallogr. D Biol. Crystallogr. 50 (1994) 760–763.
[79] G.N. Murshudov, A.A. Vagin, E.J. Dodson, Refinement of macromolecular structures by the maximum-likelihood method, Acta Crystallogr. D 53 (1997) 240–255.
[80] P. Emsley, K. Cowtan, Coot: model-building tools for molecular graphics, Acta Crystallogr. D Biol. Crystallogr. 60 (2004) 2126–2132.
[81] A.L. Morris, M.W. MacArthur, E.G. Hutchinson, J.M. Thornton, Stereochemical quality of protein structure coordinates, Proteins 12 (1992) 345–364.
[82] M.A. Parry, S.R. Stone, J. Hofsteenge, M.P. Jackman, Evidence for common structural changes in thrombin induced by active-site or exosite binding, Biochem. J. 290 (Pt 3) (1993) 665–670.
[83] Q.D. Dang, M. Sabetta, E. Di Cera, Selective loss of fibrinogen clotting in a loop-less thrombin, J. Biol. Chem. 272 (1997) 19649–19651.
[84] A. Bah, Z. Chen, L.A. Bush-Pelc, F.S. Mathews, E. Di Cera, Crystal structures of murine thrombin in complex with the extracellular fragments of murine protease-activated receptors PAR3 and PAR4, Proc. Natl. Acad. Sci. USA 104 (2007) 11603–11608.
[85] L.A. Bush, R.W. Nelson, E. Di Cera, Murine thrombin lacks Na+ activation but retains high catalytic activity, J. Biol. Chem. 281 (2006) 7183–7188.
[86] F. Marino, Z.W. Chen, C. Ergenekan, L.A. Bush-Pelc, F.S. Mathews, E. Di Cera, Structural basis of Na+ activation mimicry in murine thrombin, J. Biol. Chem. 282 (2007) 16355–16361.
[87] S.M. Wilbanks, D.B. McKay, How potassium affects the activity of the molecular chaperone Hsc70: II. Potassium binds specifically in the ATPase active site, J. Biol. Chem. 270 (1995) 2251–2257.
[88] M.T. Lai, E. Di Cera, J.A. Shafer, Kinetic pathway for the slow to fast transition of thrombin. Evidence of linked ligand binding at structurally distinct domains, J. Biol. Chem. 272 (1997) 30275–30282.
[89] E.R. Guinto, E. Di Cera, Large heat capacity change in a protein–monovalent cation interaction, Biochemistry 35 (1996) 8800–8804.
[90] A. Fontana, M. Zambonin, P. Polverino de Laureto, V. De Filippis, A. Clementi, E. Scaramella, Probing the conformational state of apomyoglobin by limited proteolysis, J. Mol. Biol. 266 (1997) 223–230.
[91] E. Di Cera, A structural perspective on enzymes activated by monovalent cations, J. Biol. Chem. 281 (2006) 1305–1308.
[92] C.H. Suelter, Enzymes activated by monovalent cations, Science 168 (1970) 789–795.